AIP | Review of Scientific Instruments

Investigations of protons passing through the CR-39/PM-355 type of solid state nuclear track detectors

A. Malinowska, A. Szydłowski, M. Jaskóła, A. Korman, B. Sartowska et al.

Citation: Rev. Sci. Instrum. **84**, 073511 (2013); doi: 10.1063/1.4815833
View online: http://dx.doi.org/10.1063/1.4815833
View Table of Contents: http://rsi.aip.org/resource/1/RSINAK/v84/i7
Published by the AIP Publishing LLC.

Additional information on Rev. Sci. Instrum.

Journal Homepage: http://rsi.aip.org
Journal Information: http://rsi.aip.org/about/about_the_journal
Top downloads: http://rsi.aip.org/features/most_downloaded
Information for Authors: http://rsi.aip.org/authors

ADVERTISEMENT

Downloaded 02 Sep 2013 to 131.188.201.33. This article is copyrighted as indicated in the abstract. Reuse of AIP content is subject to the terms at: http://rsi.aip.org/about/rights_and_permissions

Investigations of protons passing through the CR-39/PM-355 type of solid state nuclear track detectors

A. Malinowska,[1,a)] A. Szydłowski,[1] M. Jaskóła,[1] A. Korman,[1] B. Sartowska,[2] T. Kuehn,[3] and M. Kuk[1]

[1]*National Centre for Nuclear Research, Andrzeja Sołtana 7 str., Otwock 05-400, Poland*
[2]*Institute of Nuclear Chemistry and Technology, Dorodna 16 str., Warsaw 03-195, Poland*
[3]*Physikalisches Institut, Universität Erlangen – Nürnberg, D-91058, Erlangen, Germany*

(Received 27 December 2012; accepted 1 July 2013; published online 24 July 2013)

Solid State Nuclear Track Detectors of the CR-39/PM-355 type were irradiated with protons with energies in the range from 0.2 to 8.5 MeV. Their intensities and energies were controlled by a Si surface barrier detector located in an accelerator scattering chamber. The ranges of protons with energies of 6–7 MeV were comparable to the thickness of the PM-355 track detectors. Latent tracks in the polymeric detectors were chemically etched under standard conditions to develop the tracks. Standard optical microscope and scanning electron microscopy techniques were used for surface morphology characterization. © *2013 AIP Publishing LLC*. [http://dx.doi.org/10.1063/1.4815833]

I. INTRODUCTION

During the last 40 years the method generally known as Solid State Nuclear Track Detector (SSNTD) has grown and is now a distinct branch of science and technology. Fields where well-established applications of this technique already exist include nuclear physics, space physics, cosmic ray physics, particle accelerator physics, geology and archaeology, medicine and biology, radiation protection studies for space research, and – in particular – high temperature plasma studies.[1]

Some properties of SSNTDs, such as their high sensitivity to ions over a wide energy range, their nearly 100% detection efficiency for charged projectiles, the ability to register relatively high particle fluxes, resistance to vacuum conditions, very small sensitivity to photons and electrons make them very useful tools for hot plasma experiments. Therefore, one can observe an increasing interest in such detectors in many plasma laboratories.[2–4]

At the Andrzej Soltan Institute for Nuclear Studies (SINS) now the National Centre for Nuclear Research (NCNR), CR-39 track detectors and recently PM-355 derivatives of the CR-39 material ($C_{12}H_{18}O_7$) have been used for a long time. Calibration studies of the aforementioned detectors have also been performed at SINS for several years. As a result of these studies we obtained an extensive collection of data on the shapes of tracks formed by different projectiles at various energies.[5,6] The problem of the development and simulation of etched track profiles in CR-39 material and comparison with experimental results for light ions of different kinds and energies has been the subject of many studies in recent years.[7–13] The currently existing computer programs calculate the depth, diameter, range, saturation time, and etch rates versus etching time. The simulation programs reasonably approximate the experimental three dimensional track images for protons, α particles, and Li ions. But further experimental data on bulk etch rate values V_B and depth of tracks L(t) would help in developing models that better fit the experimental observations.

This paper presents the results of our recent measurements of the changes in track diameters D(t), as well as in the geometry of proton track openings at the entrance and exit surfaces of the plastic. The results of our study of the sensitivity function $V = V_T/V_B$ as a function of proton energy and etching time t are also demonstrated in this paper. The main aim of this work was to determine the shape of proton tracks near the end of the projectile range in the detector material. The proton energies (6–7 MeV) were chosen to give a proton range in the polymer of about 500 μm to be near the Bragg peak.

II. EXPERIMENT

In this paper SSNTDs of the CR-39/PM-355 type with a thickness of 0.5 mm were exposed to protons with energies in the interval 0.2–8.5 MeV.[14] To perform the calibration measurements, rectangular samples were irradiated by protons elastically scattered from a thin Au foil. Proton beams were delivered by two accelerators. In the energy range from 0.2 MeV up to 2.0 MeV the irradiation was performed with steps of about 0.2 MeV using the "Lech" Van de Graaff accelerator at NCNR, Poland. Higher energy protons, i.e., with energies from 2.0 MeV to 8.5 MeV changed in steps of about 0.3 MeV, were provided by the Tandem accelerator operated at the Erlangen-Nürnberg University, Germany. The accelerated protons, after scattering on about 130 μg/cm^2 thick gold foil, hit at almost normal incidence the SSNTD samples with up to about 3×10^4 particles/cm^2. At each energy six rectangular samples ($\sim 1 \times 3$ cm^2) cut from the same production sheets were simultaneously irradiated. The scattered protons were monitored with a Si surface–barrier detector located at 150° relative to the incident proton beam in order to determine their energy spectra and to control the counting rate. The energy spread of the elastically back–scattered protons depends mainly on the total energy loss in the target (Au foil)

a)a.malinowska@ncbj.gov.pl

 © 2013 AIP Publishing LLC

Downloaded 02 Sep 2013 to 131.188.201.33. This article is copyrighted as indicated in the abstract. Reuse of AIP content is subject to the terms at: http://rsi.aip.org/about/rights_and_permissions

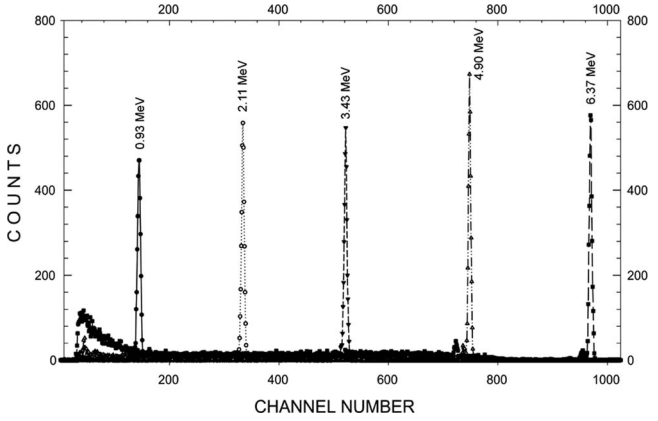

FIG. 1. Spectra of back-scattered protons on a thin Au target as measured by means of a Si detector located at an angle of 150° relative to the incident proton beam. The back scattered proton spectra at higher incident proton energies (about 5 MeV) indicate worse quality. This is caused by the multiscattering of protons by slits, collimators, beam tube, etc. In the spectra at higher incident proton energies some nuclear reaction products can also be present [from (p, p′), (p, d), (p, t), (p, α) nuclear reactions].

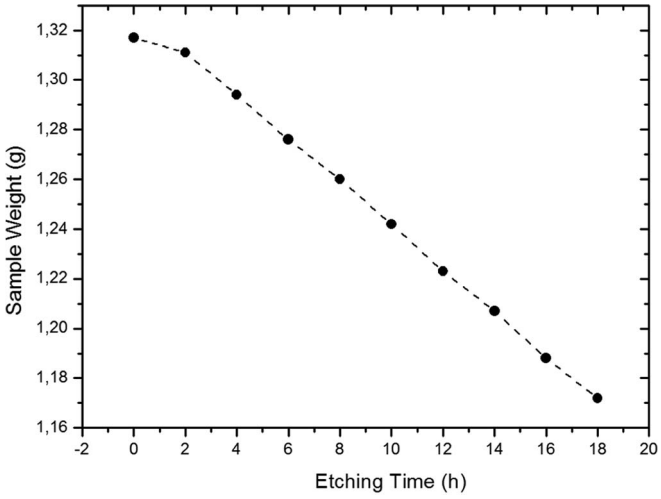

FIG. 2. The weight losses after every 2 h etching procedure of a 20.1 cm^2 piece of the non-irradiated PM-355 sample. The broken line is drawn to guide the eye.

and it ranges from 40 keV for 2 MeV protons up to 30 keV for 8 MeV protons. Typical energy spectra of the back scattered protons that hit the SSNTD samples and measured by the Si detector are shown in Fig. 1.

After the irradiation, samples were chemically etched in steps in a 6.25 N water solution of NaOH at a temperature of 70 °C ± 1 °C during selected time intervals. The etching process was performed with the samples attached to a special rotating holder made of Teflon. The rotation of the samples keeps the homogeneity of the etching solution and prevents the deposition of etch products on the detector surfaces. In the first step one part of the irradiated PM-355 samples were analyzed in order to determine track diameter magnitudes versus proton energies and etching time t. The track detector read-out was made using a semiautomatic system composed of an optical microscope connected to a PC by means of a CCD camera and suitable software (Nikon-NIS-Elements BR 4.00.03-64 bit). In the second step an electron microscope (SEM) was used to measure the track length L(t) as a function of etching time. A scanning Electron Microscope of DSM 942 type (Zeiss, Germany) was the main tool used to study the surface morphology of the detectors irradiated with protons with energies of 6–7 MeV. Both detector surfaces – projectile entrance and exit sides – were examined for track diameter measurements with statistics of about 50 events. Fractures of the detectors were observed for determination of the track shape and depth. Samples for SEM observations were prepared with a procedure carried out for non-conductive samples: conductive glue and covering with a thin gold layer.[15,16]

III. RESULTS AND DISCUSSION

The widely accepted growth models of the track etch-pit involve two etch rates: the track etch rate along the particle trajectory (V_T) and the material bulk etch rate (V_B). The latent track develops into a conical etch pit when the track etching velocity V_T is larger than the bulk etching velocity V_B.[5,17] The values of the bulk etch rates were determined in our all experiments from the weight losses of rectangular samples with areas between 15 and 21 cm^2 of non irradiated PM-355 detector material which were subjected to the interrupted etching procedure. The same etching conditions were used in all our measurements (i.e., a 6.25 N water solution of NaOH at a temperature of 70 °C). Figure 2 presents the weight losses of our detector material after every 2 h etching.

One can observe that the detector material is removed with two bulk etching rates, V_B. In the first hour of etching time we found a bulk etch rate V_B equal to 0.60 ± 0.12 μm/h, while from the next 8 × 2 h measurements of the detector we obtained a linear relation between the loss of the detector weight values and the etching time and an almost constant V_B value equal to 1.65 ± 0.2 μm/h. Also, the density of the detector material was determined by a weighing method and was equal to about 1.26 g/ cm^3. Such V_B behavior was also observed by other authors, i.e., Yamamoto *et al.*[18] They found a smaller V_B value in the first 750 nm layer and a higher V_B for deeper than 750 nm layers. These authors suggest that the probable cause of this phenomenon is the hardness of the surface layer of the detector, which was in contact with the casting glass plate during the manufacturing procedure.

The bulk etch rate determined using three independent experimental methods, by Dörschel *et al.*[8] gives a mean value of V_B = 1.83 μm/h in comparison to our lower value of V_B = 1.65 μm/h, resulting from a lower concentration of NaOH water solution for sample etching. Hermsdorf used a V_B value of 1.73 ± 0.09 μm/h, the accuracy of which was checked and verified by an international team in laboratories in Germany, France, and Japan.[19,20] The latter values are also higher because of the higher concentration of the NaOH solution relative to ours.

It is also important to note that our earlier measurements of V_B carried out during the relatively long period of about 15 years indicated different values.[21] The V_B values of PM-355 detector materials purchased before 2000 appeared to be smaller (about 1.5 ± 0.2 μm/h) than similar values of PM-355 detectors which were bought after 2005. Also Fromm[10]

Downloaded 02 Sep 2013 to 131.188.201.33. This article is copyrighted as indicated in the abstract. Reuse of AIP content is subject to the terms at: http://rsi.aip.org/about/rights_and_permissions

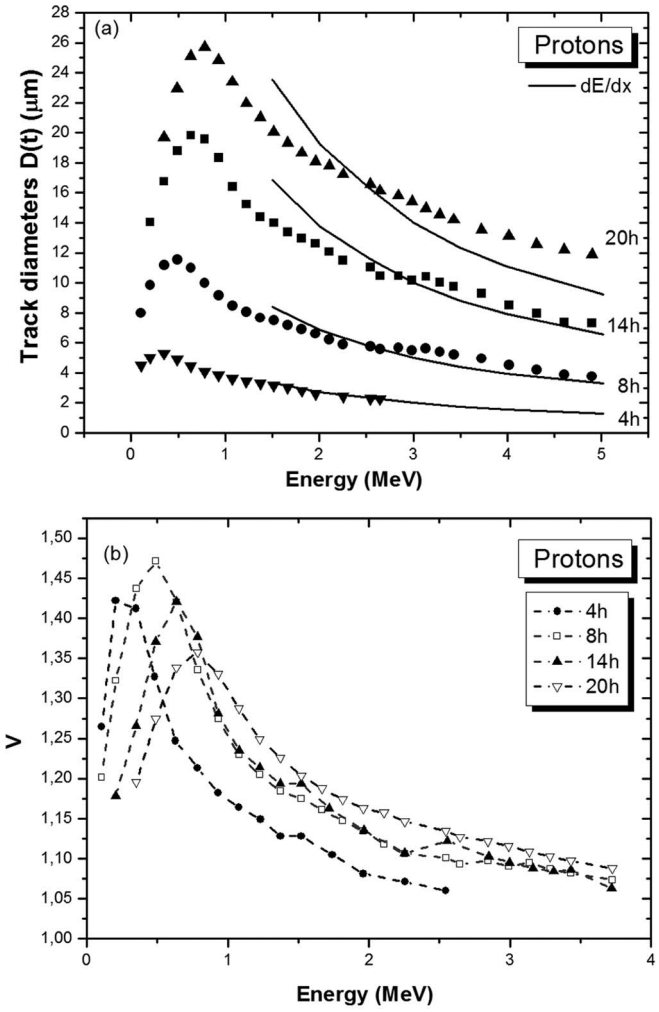

FIG. 3. (a) Evolution of track diameters as a function of incident proton energy and etching time. The solid lines represent the dE/dx dependence. This curve is normalized to the experimental data at proton energy equal to 2 MeV. (b) The track registration sensitivity function $V = V_T/V_B$ versus energy and etching time t. Broken lines are drawn to guide the eye.

noticed that V_B can vary from one experiment to another, even if the same detector material as well as etching conditions (solution concentration, temperature, and etching time) are used. Azooz *et al.*[12] also found that the bulk etching rate of the CR-39 material achieved values between 1.32 and 1.43 μm/h for the same etching conditions as were used in our studies. In most codes which simulate the track profiles, the bulk etch rates, V_B, are assumed to have constant values (time independent). According to the observation demonstrated in our present paper and the paper by Yamamoto *et al.*[13] a constant value of V_B can be assumed only after a few hours of etching.

In Fig. 3(a) we assemble the results of the detailed calibration measurements which were performed for protons, i.e., track diameters D(t) versus proton energy and 4, 8, 14, and 20 h etching time values. The diagrams demonstrate specific maxima, which are shifted to higher proton energy for longer etching times.

Our earlier studies showed that the location of the maximum is defined by the thickness of the external detector layer removed during the bulk etching process and the range of the projectile in the detector material.[5,22] This means that the tracks are etched out to the largest diameters only when the etching solution has unconstrained access to the end part of the particle trajectory where the concentration of the detector material defects is the highest. This takes place after removal by etching of the external layer of thickness equal to the projectile range. As illustrated in Fig. 3(a), the track diameters increase very fast in the region of relatively low proton energy. When the maximum is attained the track diameters decrease monotonically with a further increase in proton energy. In the region 1 MeV–6 MeV track diameter magnitudes decrease approximately as expected from the stopping power energy dependence (shown as the solid line in Fig. 3(a)).

The track registration sensitivity function $V = V_T/V_B$ was obtained on the basis of the results of the track diameter measurements D(t) which are presented in Fig. 3(a). The track etch rate V_T was calculated using the standard method proposed by Fleischer *et al.*[23] The approximate formula for V_T was derived assuming conical track profiles. Such an assumption is additionally confirmed by our measurements of the track profiles presented in Fig. 6. This formula has the form

$$V_T = V_B \frac{1 + (D(t)/2 \cdot V_B \cdot t)^2}{1 - (D(t)/2 \cdot V_B \cdot t)^2}. \quad (1)$$

The values of the sensitivity function obtained are presented in Fig. 3(b). From Fig. 3(b) one can see that the sensitivity function V(t) is systematically shifted to higher energies with increasing etching time. The reason for such a shift can be explained by the data presented in a series of publications by the group from Dresden University of Technology, Germany, but particularly on the basis of data presented in Fig. 10 of Dörschel *et al.* where the track etch rate V_T as a function of etching time in the proton energy range 0.77–7.08 MeV is shown.[8,24,25] The track etch rate V_T dependence versus etching time t published by Dörschel *et al.*[8] shows a classical analog of the Bragg curves. The maximum values of V_T occur at the depths where the proton energy loss has its maximum values. On the basis of Fig. 10 published by Dörschel *et al.* we can say that at a fixed etching time all curves V_T are cut-off.[8] For high proton incident energies the long tail of the Bragg curves is crossed. For lower energies this crossing reaches the Bragg peak region more and more and consequently the sensitivity function V increases with decreasing energy up to a maximum value. This maximum shifts with increasing etching time.

The proton range and stopping power in PM-355 material were calculated using the computer code TRIM of Ziegler *et al.*, and the results obtained are presented in Figs. 4(a) and 4(b).[26]

To study the track evolution in the reverse direction (i.e., towards the exit side) we had to choose incident projectiles of a range comparable with the detector thickness. In the present experiment we used detectors of thickness about 500 μm. Such a thickness is comparable to the range of incident protons with energies equal to 6–7 MeV. Transmission measurements as performed for 8.3 MeV protons in our PM-355 detector samples showed that these protons lost about 5 MeV energy penetrating through the sample, which could indicate that the sample was in reality about 490 μm thick. Thickness measurements performed using a mechanical

Downloaded 02 Sep 2013 to 131.188.201.33. This article is copyrighted as indicated in the abstract. Reuse of AIP content is subject to the terms at: http://rsi.aip.org/about/rights_and_permissions

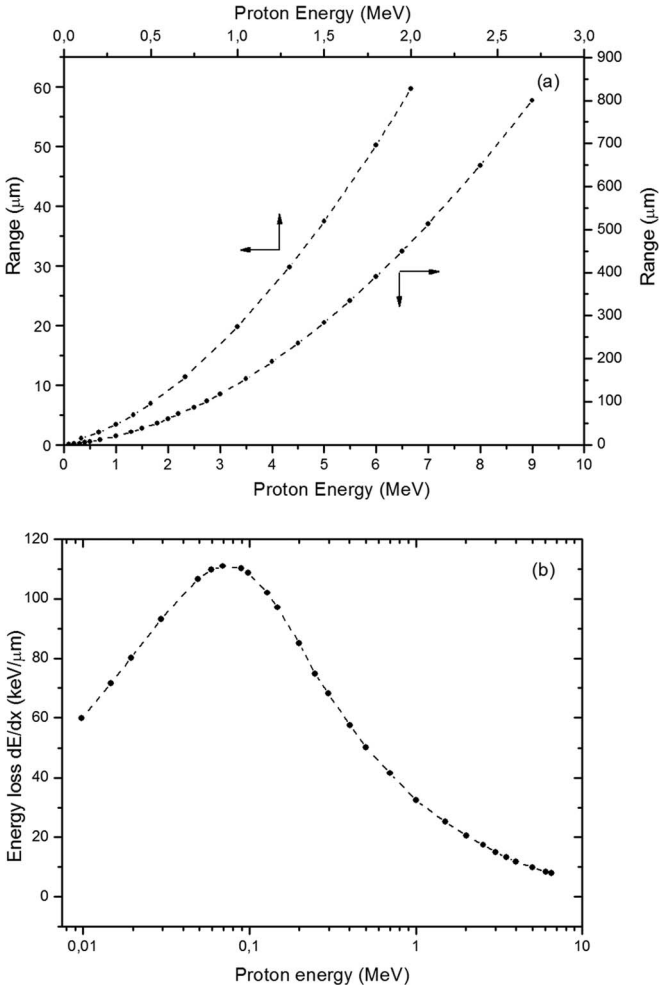

FIG. 4. (a) Proton ranges in the PM-355 detector for 1.3 g/cm^3 density value of the detector material. Broken lines are drawn to guide the eye. (b) Proton stopping power in the PM-355 ($\rho = 1.3$ g/cm^3). The broken line is drawn to guide the eye.

micrometer (with a few μm accuracy) showed similar values. This measurement also revealed that the samples were not homogeneously thick.

In Fig. 5 we present diagrams of track diameter evolution D(t) measured at the entrance and exit sides of a PM-355 detector irradiated by protons with energies: 6.36, 6.66, and 7.25 MeV as a function of etching time using the scanning electron microscopy (SEM) technique. In the case of protons with the smallest energy, i.e., 6.36 MeV (Fig. 5(a)), no tracks were developed at the exit side after 1, 2, and 3 h of etching. The first tracks developed at the exit side of the sample appeared after 4 h, i.e., when the thickness of the detector layer removed from one side of the detector sample was equal to about 6 μm. This means that the projectile was slowed down inside the polymer and didn't pass across the whole detector and stopped shortly before the exit side. In the case of protons with higher incident energy, 6.66 MeV (Fig. 5(b)), tracks were developed on both sides and visible after the first hour's etching.

This means that the projectiles penetrate the detector and the etching solution starts the etching process of the track immediately on both sides of the sample. The exit residual energy is about 1.5 MeV. The etching process at the exit side takes place in the Bragg peak region (Fig. 4(b)) where the stopping power is higher than at the entrance side for an incident proton energy of 6.66 MeV. In consequence the track diameters are larger at the exit side because the track diameters are correlated with the stopping power values (shown

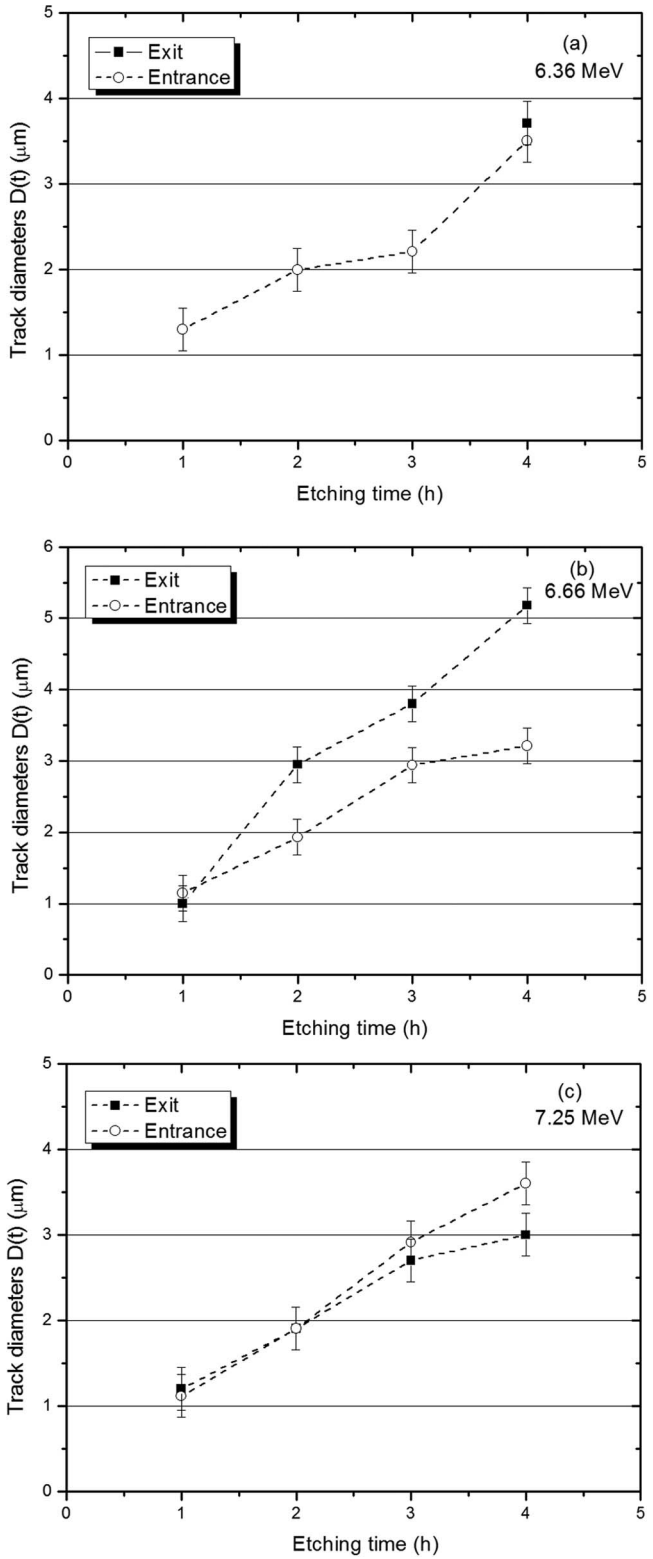

FIG. 5. Diagrams of the track diameter evolution at the entrance and exit sides of the PM-355 detector irradiated by 6.36, 6.66, and 7.25 MeV protons as a function of etching time. Lines are drawn to guide the eye.

Downloaded 02 Sep 2013 to 131.188.201.33. This article is copyrighted as indicated in the abstract. Reuse of AIP content is subject to the terms at: http://rsi.aip.org/about/rights_and_permissions

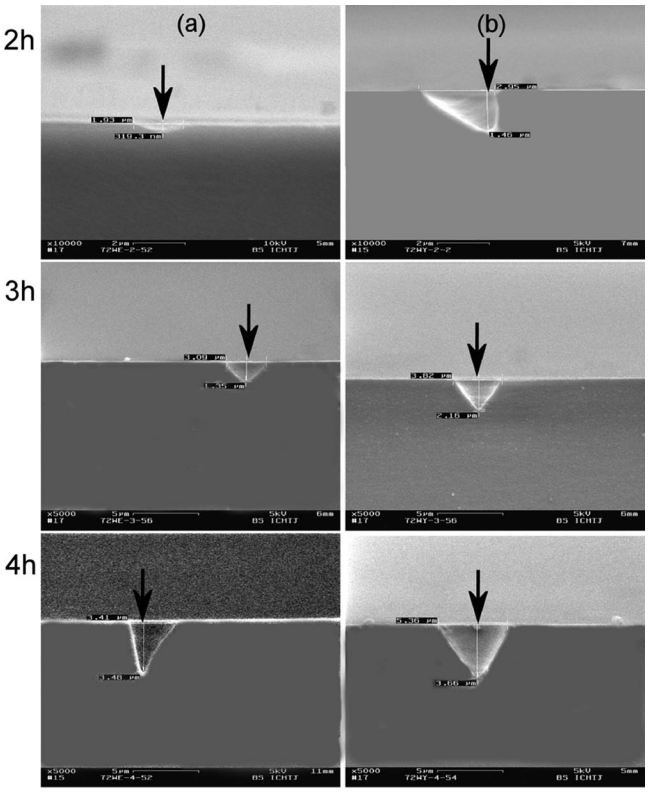

FIG. 6. Evolution of the shape of tracks caused by 6.66 MeV protons as observed after etching times of 2, 3, and 4 h: (a) at entrance and (b) at exit sides of the PM-355 detector. Arrows indicate the projectile path.

schematically in Fig. 3(b)). Finally, for protons with energy 7.25 MeV (see Fig. 5(c)) the projectile penetrates the detector with a residual energy of about 2–3 MeV. The etching process starts at relatively high projectile energy on the exit side. Since the difference in the stopping power values at the exit and entrance sides is small the track diameters on the entrance side are only slightly different and smaller from those on the exit side.

The shape evolution of the entrance and exit tracks induced by 6.66 MeV protons in the PM-355 detectors is presented in Fig. 6 versus etching time.

Developed tracks are conical in shape (and their depths at both sides of the detector were measured using the scanning electron microscope). On the basis of the track depth L(t) measurement results and the V_B values determined in this paper the V_T values at the entrance and exit sides of the detector were calculated using the formula (2) presented in papers by Hermsdorf, and by Balestra *et al.*, which was originally proposed by Dörschel *et al.*:[17,25,27]

$$V_T = dL/dt + V_B. \tag{2}$$

One can note that the response function at the exit side of the detector is higher than at the entrance side (see Figs. 7(a) and 7(b)). It is plausible to note that the track depths L(t) on the exit side are larger due to the smaller exit proton energy and in consequence the larger value of the stopping power. In Fig. 7(c) we also present the V_T values at the entrance and exit sides of the detector for 6.66 MeV protons obtained from the track diameters D(t) presented in Fig. 5(b) and measured using the scanning electron microscope technique.

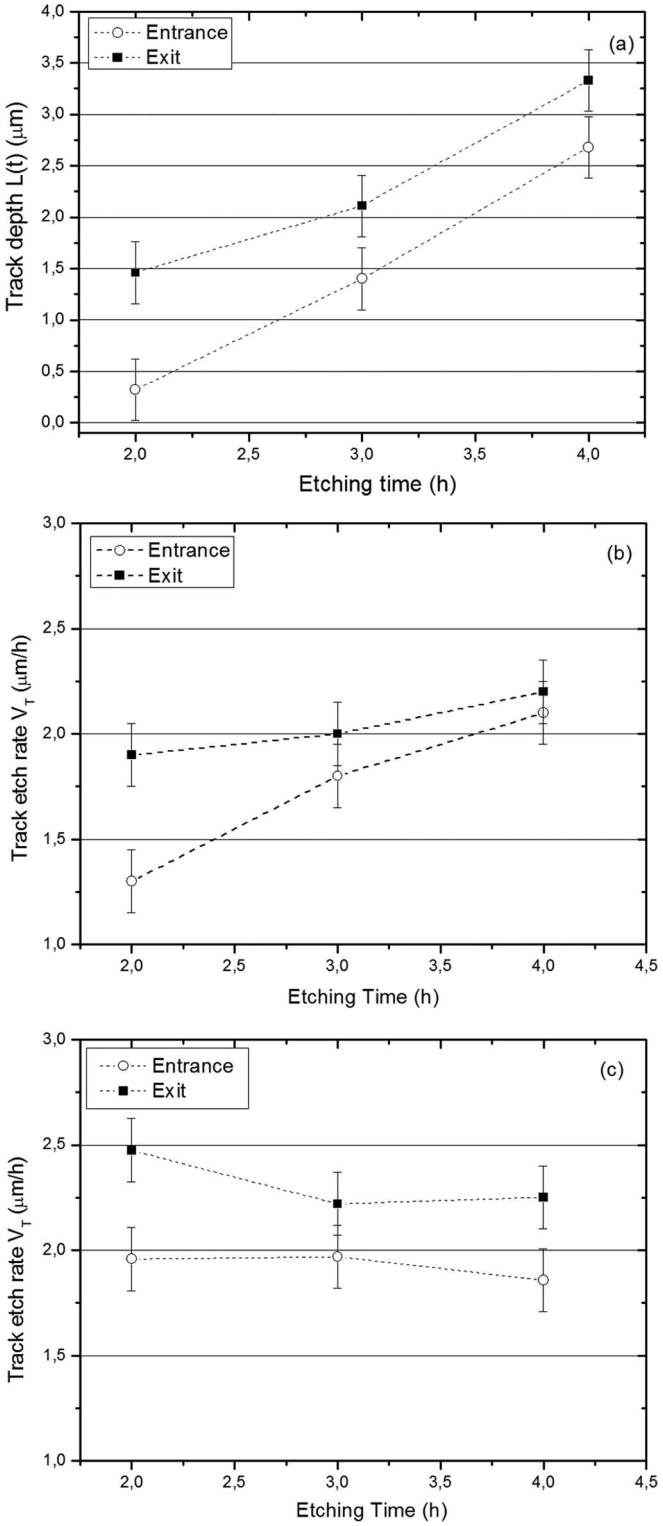

FIG. 7. (a). The track depth versus etching time for entrance and exit sides of the PM-355 samples for 6.66 MeV protons. Broken lines are drawn to guide the eye. (b). V_T etch rate values versus etching time for entrance and exit sides of the PM-355 samples for 6.66 MeV protons obtained from track depth L(t). Broken lines are drawn to guide the eye. (c). V_T etch rate values versus etching time for entrance and exit sides of the PM-355 samples for 6.66 MeV protons obtained from track diameters D(t) presented in Fig. 5(b). Broken lines are drawn to guide the eye.

These V_T values were calculated using formula (1). Comparing the V_T values presented in Figs. 7(b) and 7(c) one can see that the V_T values calculated using D(t) are slightly

Downloaded 02 Sep 2013 to 131.188.201.33. This article is copyrighted as indicated in the abstract. Reuse of AIP content is subject to the terms at: http://rsi.aip.org/about/rights_and_permissions

higher in comparison to the V_T values obtained from the track length L(t) but agree with the experimental errors to within 10%–20%. According to the work of Hermsdorf the V_T values obtained on the basis of D(t) and L(t) for the same etching time cannot agree because of the general dependence of V_T (x) on the depth x along the particle trajectory in the detector.[25]

Observations of diameters and shapes of tracks in direct and reverse directions recently carried out by Hermsdorf and Hunger[7] indicate the dependence of track geometry on the stopping power values (Bragg peak).

IV. CONCLUSIONS

The most important results of these studies can be summarized as follows:

1. Two phases of the bulk etch rate V_B value were observed: 0.60 μm/h $\pm$ 0.1 (smaller) in the near surface layer—around 1 μm and 1.65 μm/h $\pm$ 0.2 (higher), almost constant, in the deeper layers of the detector used here.
2. For optimal etching conditions the pre-etching procedure before irradiation of the SSNTD samples will be very useful for eliminating the near surface bulk etch rate V_B and also to reduce the surface background of the samples.
3. The slope of the track diameter evolution in the energy range 1–6 MeV is correlated with the stopping power dependence.
4. From the measurements carried out it can be noted that the diameters and the depths of the tracks are higher at the exit side of the detector for protons with 6.66 MeV energy than at the entrance side of the detector used here.
5. Observations of the diameter and shape of developed tracks at the entrance and exit side of the PM-355 detector allowed us to verify the theory of increasing energy loss for charged projectiles near the point of their range in the detector material.
6. The use of the high resolution scanning electron microscopy (SEM) technique enabled us to measure geometrical parameters of small tracks (after a short etching time) especially for protons (e.g., track diameters D(t) and track depths L(t)).
7. Using the SEM technique for the determination of the track profile has several limitations: it is time consuming, destructive, and in practice it is difficult to obtain good statistics.
8. The V_T values, obtained by two different methods, from track diameter D(t) and track length L(t) of the etched tracks are in good agreement, in the limit of an acceptable margin of errors.

ACKNOWLEDGMENTS

We would like to thank Dr. N. Keeley for a critical reading of the manuscript and for constructive suggestions.

[1] S. A. Durrani, "Nuclear tracks: A success story of the 20th century," Radiat. Meas. **34**(1–6), 5–13 (2001).
[2] N. Sinenian, M. J. Rosenberg, M. Manuel, S. C. McDuffee, D. T. Casey, A. B. Zylstra, H. G. Rinderknecht, M. Gatu Johnson, F. H. Seguin, J. A. Frenje, C. K. Li, and R. D. Petrasso, Rev. Sci. Instrum. **82**, 103303 (2011).
[3] K. Malinowski, E. Składnik-Sadowska, M. J. Sadowski, and K. Czaus, Radiat. Meas. **44**, 865 (2009).
[4] J. Badziak, S. Jabłoński, M. Kubkowska, P. Parys, M. Rosiński, J. Wołowski, A. Szydłowski, P. Antici, J. Fuchs, and A. Mancic, Radiat. Eff. Defects Solids **165**, 760 (2010).
[5] A. Szydłowski, M. Sadowski, T. Czyżewski, M. Jaskóła, A. Korman, and I. Fijał, Nucl. Instrum. Methods Phys. Res. B **171**, 379 (2000).
[6] B. Sartowska, A. Szydłowski, M. Jaskóła, and A. Korman, Radiat. Meas. **40**, 347 (2005).
[7] D. Hermsdorf and M. Hunger, Radiat. Meas. **44**, 766 (2009).
[8] B. Dörschel, D. Fülle, H. Hartmann, D. Hermsdorf, K. Kadner, and Ch. Radlach, Radiat. Prot. Dosim. **69**, 267 (1997).
[9] D. Hermsdorf and U. Reichelt, Radiat. Meas. **45**, 1000 (2010).
[10] M. Fromm, Radiat. Meas. **40**, 160 (2005).
[11] A. A. Azooz, S. H. Al-Nia'emi, and M. A. Al-Jubbori, Radiat. Meas. **47**, 67 (2012).
[12] A. A. Azooz, S. H. Al-Nia'emi, and M. A. Al-Jubbori, Comput. Phys. Commun. **183**, 2470 (2012).
[13] D. Nikezic, D. Kostic, C. W. Y. Yip, and K. N. Yu, Radiat. Meas. **41**, 253 (2006).
[14] Catalog Page Pershore Moulding Company, 1998.
[15] J. I. Goldstein, D. E. Newbury, P. Echlin, D. C. Joy, Jr., Roming, C. E. Lyman, C. Fiori, and E. Lifshin, *Scanning Electron Microscopy and X-Ray Microanalysis. A Text for Biologist, Materials Scientists, and Geologists* (Plenum Press, New York and London, 1992).
[16] O. L. Orelovitch, P. Yu Apel, and B. Sartowska, J. Microsc. **224**, 100 (2006).
[17] S. Balestra, M. Cozzi, G. Giacomelli, R. Gicomelli, M. Giorgini, A. Kumar, G. Mandrioli, S. Manzoor, A. R. Margiotta, E. Madinaceli, L. Patrizzi, V. Popa, I. E. Quereshi, M. A. Rana, G. Sirri, M. Spurio, Togo, and C. Valieri, Nucl. Instrum. Methods Phys. Res. B **254**, 254 (2007).
[18] D. M. Yamamoto, N. Yasuda, M. Kurano, T. Kanai, A. Furukara, N. Ishigure, and K. Ogura, Nucl. Instrum. Methods Phys. Res. B **152**, 349 (1999).
[19] D. Hermsdorf, Radiat. Meas. **44**, 806 (2009).
[20] T. Yamauchi, H. Ichijo, K. Oda, B. Dörschel, D. Hermsdorf, K. Kadner, F. Vaginay, M. Fromm, and A. Chambaudet, Radiat. Meas. **34**, 37 (2001).
[21] A. Szydlowski, B. Sartowska, A. Banaszak, J. Choiński, I. Fijał, M. Jaskóła, A. Korman, and M. J. Sadowski, Radiat. Meas. **40**, 401 (2005).
[22] A. Szydlowski, A. Malinowska, M. Jaskola, A. Korman, K. Malinowski, and M. Kuk, Radiat. Meas. **50**, 258–260 (2013).
[23] R. L. Fleischer, P. B. Price, and R. M. Walker, *Nuclear Tracks in Solids: Principles and Applications* (University of California Press, Berkeley, 1975).
[24] B. Dörschel, D. Fülle, H. Hartmann, D. Hermsdorf, K. Kadner, and Ch. Radlach, Radiat. Prot. Dosim. **71**, 99 (1997).
[25] D. Hermsdorf, Radiat. Meas. **47**, 518 (2012).
[26] J. Ziegler, J. P. Biersack, and U. Littmark, *The Stopping and Range of Ions in Solids* (Pergamon Press, New York, 1985).
[27] B. Dörschel, H. Hartmann, K. Kadner, and P. Rösler, Radiat. Meas. **25**, 157 (1995).

Downloaded 02 Sep 2013 to 131.188.201.33. This article is copyrighted as indicated in the abstract. Reuse of AIP content is subject to the terms at: http://rsi.aip.org/about/rights_and_permissions